Paper Title: Skid Prevention for EVs based on Back-EMF Observer and its Implementation to IPM Motor Driven EV

***Abstract*:** It is well-known that the separately-wound DC motor has elective torque (current) reduction characteristics in response to rapid increase of the rotational speed of the motor. This characteristic has been utilized in adhesion control of electric locomotives with DC motor. In this paper, we have proposed a new skid prevention method for EVs utilizing this characteristic and discussed the possibility of its implementation to IPM Motor Driven EV. In order to compensate for Back-EMF, disturbance observer is introduced. The experimental results of the hardware skid simulator utilizing Motor-Generator setup verified the electiveness of our proposed method.

Authors

Name (author1): Xiaoxing Liu
Affiliation/ Mailing Address: Ce-503, Institute of Industrial Science, the University of Tokyo, 4-6-1 Komaba, Meguro, Tokyo153-8505, Japan
E-mail Address (es): ryu@horilab.iis.u-tokyo.ac.jp
Phone: +81-3-5452-6289 Fax: +81-3-5452-6288

Name (author 2): Takashi Koike
Affiliation/ Mailing Address: Ce-503, Institute of Industrial Science, the University of Tokyo, 4-6-1 Komaba, Meguro, Tokyo153-8505, Japan
E-mail Address (es): koike@horilab.iis.u-tokyo.ac.jp
Phone: +81-3-5452-6289 Fax: +81-3-5452-6288

Name (author 3): Yoichi Hori
Affiliation/ Mailing Address: Ce-503, Institute of Industrial Science, the University of Tokyo, 4-6-1 Komaba, Meguro, Tokyo153-8505, Japan
E-mail Address (es): hori@iis.u-tokyo.ac.jp
Phone: +81-3-5452-6289 Fax: +81-3-5452-6288

Technical Areas
Application of Disturbance Observer

Skid Prevention for EVs based on Back-EMF Observer and its Implementation to IPM Motor Driven EV

Xiaoxing Liu,
Department of Electrical Engineering
University of Tokyo
ryu@horilab.iis.u-tokyo.ac.jp

Takashi Koike,
Department of Electrical Engineering
University of Tokyo
koike@horilab.iis.u-tokyo.ac.jp

Yoichi Hori
Department of Electrical Engineering
University of Tokyo
hori@iis.u-tokyo.ac.jp

Abstract— **It is well-known that the separately-wound DC motor has effective torque (current) reduction characteristics in response to rapid increase of the rotational speed of the motor. This characteristic has been utilized in adhesion control of electric locomotives with DC motor. In this paper, we have proposed a new skid prevention method for EVs utilizing this characteristic and discussed the possibility of its implementation to IPM Motor Driven EV. In order to compensate for Back-EMF, disturbance observer is introduced. The experimental results of the hardware skid simulator utilizing Motor-Generator setup verified the effectiveness of our proposed method.**

I. Introduction

As the next generation traffic tool, the Electric Vehicle not only has the merit of no environment pollution, but also has perfect ride performance. Because the output torque of the motor can be controlled to follow its reference value accurately, with a relatively short time constant of 1[ms] and much less dead time. There are still many challenges and chances in the research of high-performance EV[1], [2], [3].

As an excellent example making use of fast response of EVs, the separately-wound DC motor with the torque (current) reduction characteristics is researched in this paper. Our proposed skid prevention method can improve the condition between the EV and the road dramatically without any adhesion status analyzing.

II. Skid Prevention for EVs based on Back-EMF Observer

A. Vehicle Dynamic Model

Suppose that the time constant, the rolling resistance and the wind drag force are very small. The forces effecting on the vehicle are shown in Fig.1, and the dynamic equations are expressed in Equation (1) - (3).

$$\omega = \frac{1}{Js}(T - rF_d) \quad (1)$$

$$V = \frac{1}{Ms}F_d \quad (2)$$

$$V_w = r\omega \quad (3)$$

Where ω is the rotational speed of the wheel (motor), V is the speed of the vehicle, V_ω is the speed of the wheel, F_d is the driving force, T is the driving torque of the motor and s is the Laplace operator. J is the inertia moment of all the rotating parts of the EV, r is the radius of the tire and M is the mass of the EV.

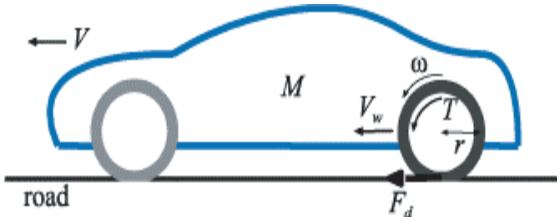

Fig. 1. Motion of vehicle

Equation (1) is the motion equation of the wheel, and the wheel is affected by the torque of the motor and the reaction force from the road. Equation (3) is the motion equation of the chassis.

B. Adhesion Characteristics of Tire and Road

The adhesion characteristics of tire and road can be expressed by the concept of slip ratio. Slip ratio λ is defined in the following equations utilizing V, V_w,

$$\lambda = \frac{V_w - V}{V_w}(Driving) \quad (4)$$

$$\lambda = -\frac{V - V_w}{V}(Braking) \quad (5)$$

Utilizing slip ratio λ, the relationship of the slip ratio and the friction coefficient μ between the tire and the road can be approximated and described, for example, by Equation (6), which is called $\mu - \lambda$ curve (function).

$$\mu = -1.05k\exp(-45\lambda) - \exp(-0.45\lambda)(Driving) \quad (6)$$

$$\mu = 1.1k\exp(35\lambda) - \exp(0.35\lambda)(Braking) \quad (7)$$

Where k is the parameter of the road status, and takes the following values, for example,

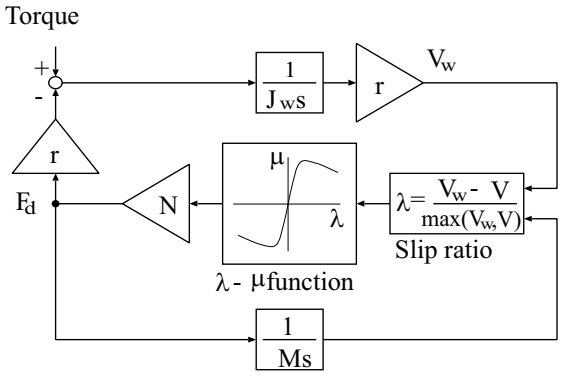

Fig. 2. Block diagram of the one-wheel vehicle model

$$k = 1(Dryroad) \quad (8)$$

$$k = 0.2(Icyroad) \quad (9)$$

After having achieved the friction coefficient μ from slip ratio λ utilizing $\mu - \lambda$ curve, the driving force F_d can be calculated by Equation (10).

$$F_d = \mu(\lambda)N \quad (10)$$

Where N is the normal component of reaction effecting on tires. The model of the one-wheel EV can be shown in Fig.2.

C. Normal Skid Prevention Scheme Utilizing Back-EMF Observer

In the condition of no speed sensor, the skid prevention controller can also be realized with other signals such as Back-EMF [**?**]. This kind of slip controller may have more reliability and more robust performance. But the signal of Back-EMF cannot be detected directly, it is necessary to set up an observer to estimate the value of Back-EMF. A current disturbance observer with variable gain and time constant is discussed in paper [5], as shown in Fig.3, which utilized the torque drop characteristic to limit the torque when slip occurs. The current disturbance observer is used to compensate the voltage drop caused by Back-EMF, so in fact it is also a Back-EMF observer.

Where G^{-1} is the inverse function of the transfer function from the voltage command v^* to the current i, which can be expressed as

$$G^{-1}(s) = \frac{JL\tau s^2 + J(L+R\tau)s + (JR+\phi^2\tau)}{J\tau s + J} + \frac{\phi^2(-k+1)}{J\tau s^2 + Js} \quad (11)$$

Following (11), G^{-1} is apparently relating to the variable gain K. When the gain K is changed, G^{-1} must be recalculated. In this paper, a novel Skid Prevention Scheme is proposed. We can adjust the variable gain K of the Back-EMF observer freely with nothing changed of the feed-forward control part.

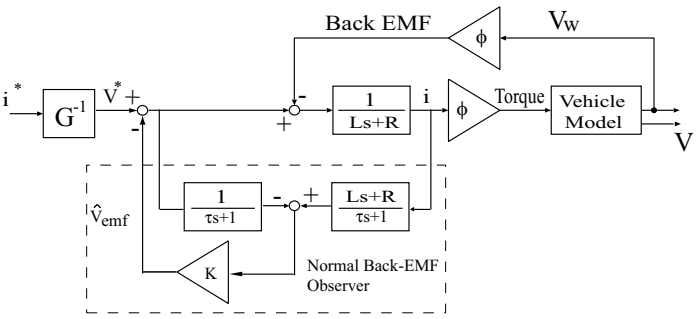

Fig. 3. The block diagram of the Back-EMF observer and the EV system installed separately wound DC motor with FF current control

D. Novel Skid Prevention Scheme

When the vehicle is running from the dry road to the icy road which is very smooth, the friction between the tire and the road is rapidly reduced. If the motor of the EV is still keeping the driving torque as before, the wheel will skid on the icy quickly. That means the Back-EMF of the motor increases instantly at the same time. In other words, we can restrain the vehicle in the safe condition by decreasing the extra increased Back-EMF.

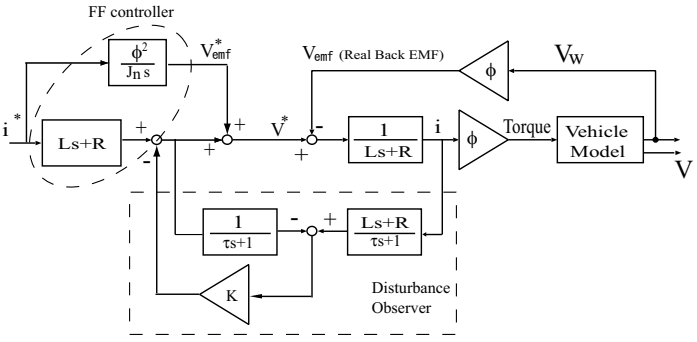

Fig. 4. Novel Skid Prevention Scheme utilizing the disturbance observer

As shown in Fig.4, in our proposed skid prevention scheme, a disturbance is utilized to estimate the extra increased Back-EMF which is evaluated by how much the real Back-EMF is bigger than the estimate value. The estimate value can be acquire as [5]

$$V_{emf} = i^* \frac{\phi^2}{J_n s} \quad (12)$$

The transfer function from the current command i^* to the current of the motor i is shown in (13).

$$\frac{i(s)}{i^*(s)} = \frac{JnL\tau s^2 + Jn(L+R\tau)s^2 + (JnR+\phi^2\tau)s}{JL\tau s^2 + J(L+R\tau)s^2 + (JR+\phi^2\tau)s} \frac{+\phi^2(1-k)}{+\phi^2(1-k)} \frac{J}{J_n} \quad (13)$$

The value of (13) is 1 because J is equal to J_n when the vehicle is in steady-state driving. Drivers can, that is to say,

control the longitudinal motion of the vehicle with abandon because the vehicle is braking or driving by the current of the motor which arbitrary current command itself becomes when the vehicle is in steady-state driving.

In the second place behaviors of the vehicle are analyzed when the vehicle skids. The inertia moment seen by the motor becomes lighter when the wheel skids than when the vehicle is in steady-state driving. In this part, the skid phenomenon is analyzed with regarding that as the phenomenon that the inertia moment J rapidly decreases. When giving the compensation gain K is 1, the final value of the step response on (13) is shown in (14) and when gain K equals other value, the step response is shown in (15), where r(t) means the step input.

$$\begin{aligned} \lim_{t\to\infty} \frac{i(t)}{i^*(t)} r(t) &= \lim_{s\to 0} s \frac{i(t)}{i^*(t)} \frac{1}{s} \\ &= \frac{J_n R + \phi^2 \tau}{JR + \phi^2 \tau} \frac{J}{J_n} (K = 1) \qquad (14) \\ &= \frac{J}{J_n} (K \neq 1) \qquad (15) \end{aligned}$$

D.1 Adjustment of Torque (Current) Reduction Characteristics with Time Constant τ

Equation (14) shows when the gain K equals 1 the transfer function from the current command i^* to the real current i depends on the time constant τ. The torque (current) reduction characteristics does not appear since the value of (14) is always 1 and the current command directly becomes the real current of the motor if the time constant τ is small enough. On the contrary, the value of (14) becomes J/J_n and the motor current becomes J/J_n times larger than the current command if the time constant τ is large enough. The simulation results are shown in the Fig.5.

In conclusion, it is proved that the torque (current) reduction characteristics can be freely adjusted by the time constant τ when the vehicle skids. It takes a little time to reduce the torque (current).

D.2 Adjustment of Torque (Current) Reduction Characteristics with Gain K

Routh 's Stability Criterion shows the condition that if K satisfies following (16) the pole equation can be kept stable.

$$1 - \frac{(L + R\tau)(JR + \phi^2 \tau)}{L\tau\phi^2} < k < 1 \qquad (16)$$

It means the time response of (13) can be freely adjusted by changing gain K only when K satisfies. In other words, it is possible to cut down the delay of the time response by adjusting gain K.

The simulation results are shown in Fig.6

Where the time constant τ is fixed $\tau = 0.001$ and gain K is changed from -1 to 1.

Fig.6(a) shows that the torque (current) reduction is quickened as gain K is enlarged to the negative direction

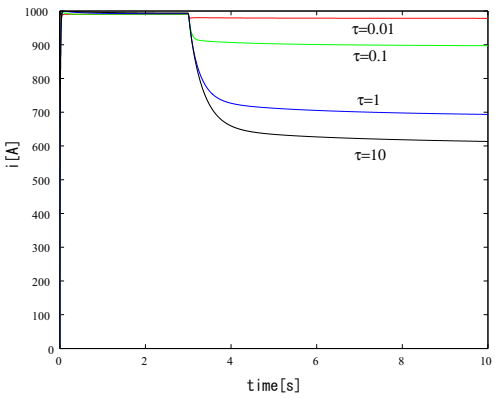

(a) The current of the motor. (The time constant τ is turned.)

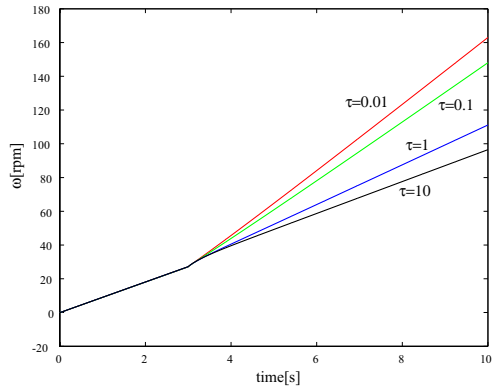

(b) The rotational speed of the motor. (The time constant τ is turned.)

Fig. 5. Adjustment of Torque (Current) Reduction Characteristics with Time Constant τ

when the vehicle skids. Fig.6(b) shows that the larger K is to the negative direction, the more the rotational speed of the motor is prevented from rapid increase.

In conclusion, it is proved that the final value of the torque when the vehicle skids is decided by the time constant of the disturbance observer and the speed of the torque (current) reduction by gain. Moreover, we can adjust both τ and K without any changing of the feed-forward control part. The most appropriate combination of both the time constant and gain in view of the destination should be considered and the torque (current) reduction characteristics be decided in order to utilize characteristics of separately-wound DC motor which prevents vehicle from skidding effectively.

E. Experimentation of Motor-Generator Setup

E.1 Outline of Experimentations

Motor-Generator setup is shown in Fig.7 and the sketch of control system is shown in Fig.8. The shafts of two motors of Motor-Generator setup are interconnected. The

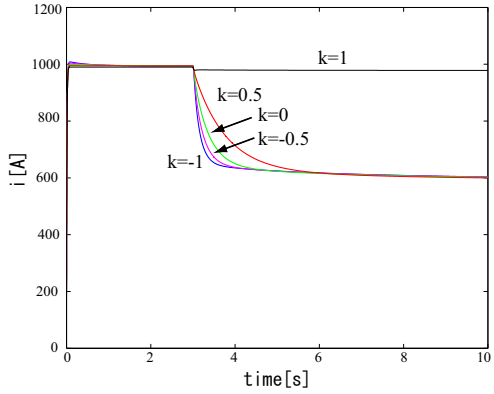

(a) The current of the motor. (The gain K is turned.)

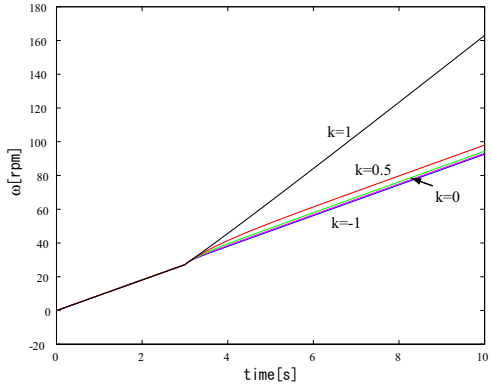

(b) The rotational speed of the motor. (The gain K is turned.)

Fig. 6. Adjustment of Torque (Current) Reduction Characteristics with gain K

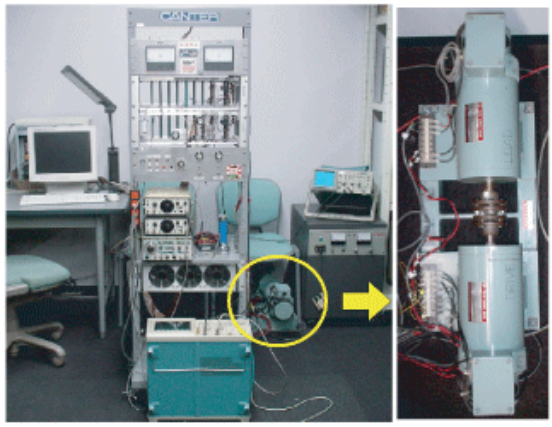

Fig. 7. Motor-Generator setup system

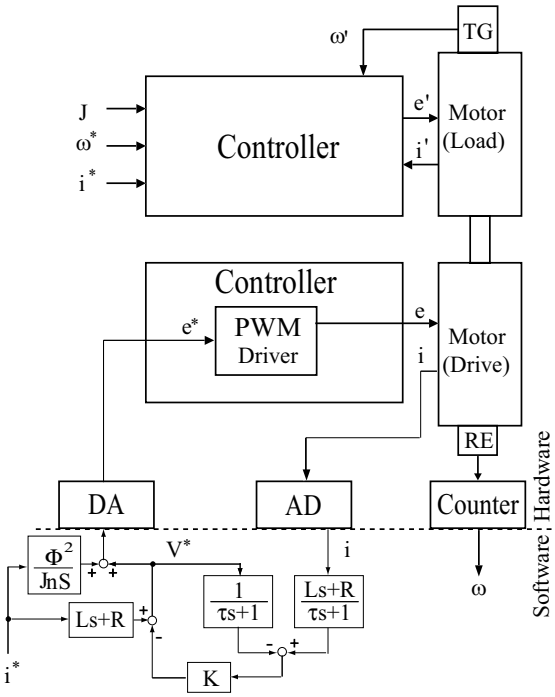

Fig. 8. Block diagram of the sontrol system utilizing Motor-Generator setup

loading motor is controlled by the only hardware control-boards and the inertia moment of the loading motor seen from the driving motor can be controlled. The driving motor is controlled by the hardware control-boards and software one. The sampling time of the software controller is $1[ms]$. The current command $i^* = 1.5[A]$, the inertia moment is rapidly decreases at about $t = 2[s]$, which means the vehicle begins to slip.

E.2 Confirmation of Torque (Current) Reduction Characteristics

The experimental test was performed in order to confirm the torque (current) reduction characteristics shown in previous section. The current of the motor and the rotational speed are observed at the accelerated speed when the vehicle slips.

The inertia moment of the motor which is simulated the skid phenomenon decreases rapidly at about $t = 2[s]$. As the same as simulation result, Fig.9(a) and Fig.10(a) show that the current of the motor reduces when the inertia moment decreases if proposed controller is being utilized. Therefore, the rotational speed of the motor is prevented from rapid increase in Fig.9(b) and Fig.10(b).

In conclusion, it proved that the proposed skid prevention method utilizing torque (current) reduction characteristic prevents vehicle equipped with separately-wound DC motor form skidding effectively.

III. Practical Experiments of Vehicle "UOT CADWELL EV" Equipped with BLDC Motors

Up to now, we have proposed a new skid prevention method for EVs, utilizing this characteristic and have made experiments with the hardware skid simulator "Motor-Generator setup". From this chapter, an implement method for applying this skid prevention control to our new vehicle "UOT CADWELL EV" equipped with BLDC

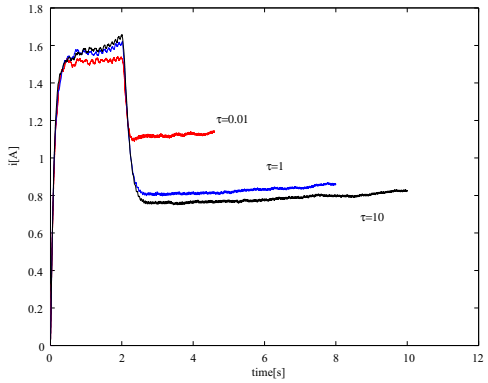

(a) The current of the motor reduces with different value of the time constant τ

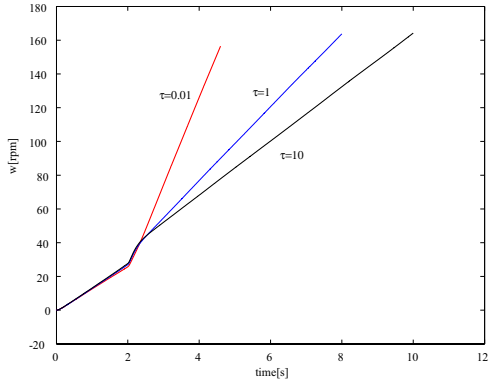

(b) The rotational speed of the motor is prevented from rapid increase with different value of the time constant τ

Fig. 9. Experimental results of the skid phenomenon with time Constant $\tau(K = 1)$

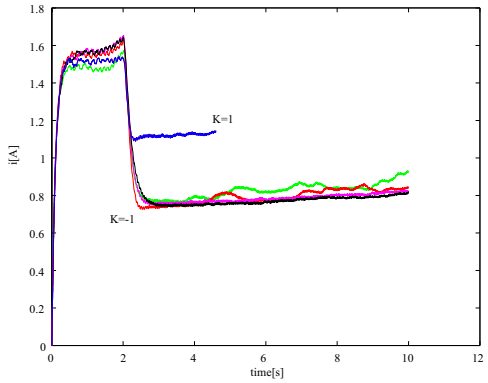

(a) Current of the motor reduces with different value of the gain K

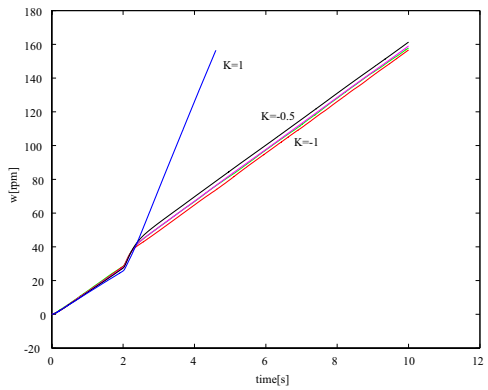

(b) Rotational speed of the motor with different value of the gain K

Fig. 10. Experimental results of the skid phenomenon with gain K $(\tau = 0.01)$

motors is proposed.

A. Vector control of BLDC motor

The equivalent circuit of BLDC motor is expressed in (17)

$$\begin{bmatrix} v_d \\ v_q \end{bmatrix} = \begin{bmatrix} R_a + pL_d & -\omega_{re}L_q \\ \omega_{re}L_d R_a & +pL_q \end{bmatrix} \begin{bmatrix} i_d \\ i_q \end{bmatrix} + \begin{bmatrix} 0 \\ \omega_{re}\psi_a \end{bmatrix} \quad (17)$$

Where R_a is armature resistance. ϕ_a is magnetic flux. d and q mean d-axis and q-axis.

In order to realize the slipping control by the proposed controller in previous chapter, two filters (Filter1, Filter2) are added composing the usual vector control of BLDC motor. Figure.11 shows the vector control configuration of the EV system equipped with BLDC motor.

B. FF+FB current control

Figure.12 shows the block diagram of the EV system equipped with decoupling controlled BLDC Motor.

In Fig.4 the relation between i^* and the voltage command v^* is shown in (18)

$$V^* = i^*(Ls + R + \frac{\phi^2}{J_n s}) + (i^* - i)(Ls + R)\frac{K}{\tau S + 1 - K} \quad (18)$$

In order to adjust torque (current) reduction by changing the time constant τ, gain K is valued 1. The block diagram of proposed skid prevention controller hybridded with PI controller is obtained as Fig.13

As shown in Fig.13, to ultilize the proposed skid prevention controller on EV system equipped with BLDC Motor, $Filter1$ is filled with G_{Filter} (19). The proportional gain K_p of the PI controller is changed to $K_p + L_q/\tau$ and the integral gain K_i changed to $K_i + R/\tau$.

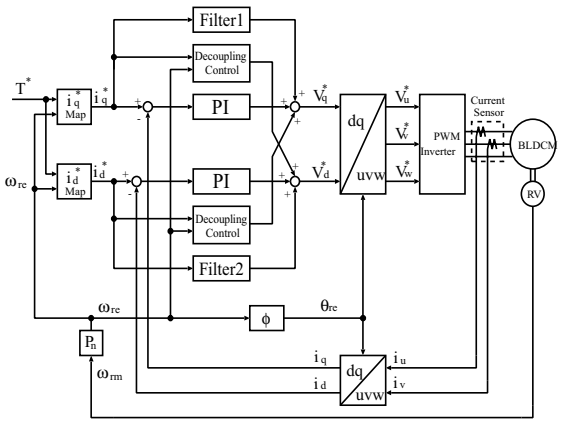

Fig. 11. Vector control configuration of the EV system equipped with BLDC motor

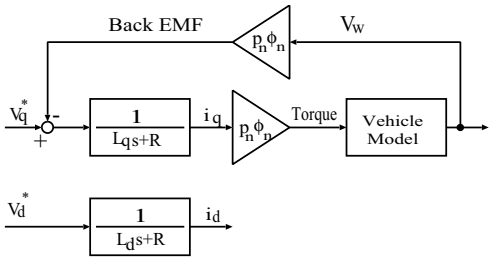

Fig. 12. Block diagram of the EV system equipped with decoupling controlled BLDC Motor

$$G_{Filter} = Ls + R + \frac{\phi^2}{J_n s} \tag{19}$$

Therefore, filter F is defined by

$$F = \begin{bmatrix} Filter1 \\ Filter2 \end{bmatrix} = \begin{bmatrix} G_{Filter} \\ 0 \end{bmatrix} \tag{20}$$

In this system, slipping is restrained by using the proposed controller for q axis utilizing torque (current) reduction characteristic in the micro time scale when slipping occurs. Though in macro time scale, the FB current control is used to output the provided torque. That is, it becomes a hybrid current control with the FF filter and FB current control. D axis that doesn't take part in calculating the torque only uses a conventional FB current control.

IV. Conclusion

The AC motor made of permanent magnet is the most appreciated and most commonly utilized for EVs at the present day and it is controlled by the high-performancecurrent controller. However because of its poor adhesion performance, this current control is shown necessary to be improved though our research.

In this paper, it proposed the traction control for EV utilizing fast torque response of electric motor. Its effectiveness has been confirmed by the experimental results

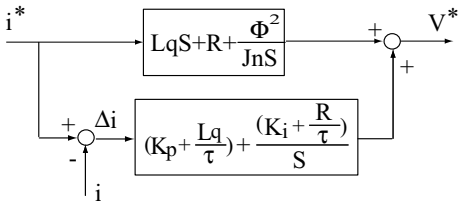

Fig. 13. Block diagram of proposed skid prevention controller hybrided with PI controller

using Motor-Generator setup and it has also been proved possible to use on "UOT CADWELL EV".

If the development of our studies comes to be utilized widely, needless to say, the risk of slip becomes dramatically small. It also can contribute greatly to safety improvement of the vehicle utilizing the advanced attitude control system even if driving on the skidding road.

References

[1] Y. Hori, "Traction Control of Electric Vehicle: Basic Experimental Results Using the Test EV UOT Electric March," IEEE Trans. on Industry Applications, Vol. 34, No. 5, pp.1131-1138, 1998.

[2] S. Sakai and Y. Hori, "Advantage of Electric Motor for Anti Slip Control of Electric Vehicle," EPE Journal, Vol.11, No.4, pp.26-32, 2001.

[3] S. Matsugaura, et al., "Evaluation of Performances for the In-Wheel Drive System for the New Concept Electric Vehicle KAZ," in Proc. EVS19, Pusan, Korea, 2002.

[4] T. Miyamoto and Y. Hori, "Adhesion Control of EV Based on Disturbance Observer," IEE of Japan Technical Meeting Record, IIC-00-9, pp.49-54, 2000. [In Japanese]

[5] S. Kodama, L. Li and Y. Hori, "Skid Prevention for EVs based on the Emulation of Torque Characteristics of Separately-wound DC Motor," in Proc. AMC-2004, 2004.3.25-27, Kawasaki

[6] Lianbing Li, Shinya Kodama, Yoichi Hori. Anti-Skid Control for EV Using Dynamic Model Error based on Back-EMF Observer. The 30th Annual Conference of the IEEE Industrial Electronics Society (IECON '04), Busan, Korea. 2004